Journal of
Experimental
Botany
www.jxb.oxfordjournals.org

RESEARCH PAPER

In vivo protein tyrosine nitration in *Arabidopsis thaliana*

Jorge Lozano-Juste, Rosa Colom-Moreno and José León*

Instituto de Biología Molecular y Celular de Plantas, CSIC-Universidad Politécnica de Valencia, CPI Ed. 8E, Camino de Vera s/n, 46022 Valencia, Spain

* To whom correspondence should be addressed. E-mail: jleon@ibmcp.upv.es

Abstract

Nitration of tyrosine (Y) residues of proteins is a low abundant post-translational modification that modulates protein function or fate in animal systems. However, very little is known about the *in vivo* prevalence of this modification and its corresponding targets in plants. Immunoprecipitation, based on an anti-3-nitroY antibody, was performed to pull-down potential *in vivo* targets of Y nitration in the *Arabidopsis thaliana* proteome. Further shotgun liquid chromatography–mass spectrometry (LC-MS/MS) proteomic analysis of the immunoprecipitated proteins allowed the identification of 127 proteins. Around 35% of them corresponded to homologues of proteins that have been previously reported to be Y nitrated in other non-plant organisms. Some of the putative *in vivo* Y-nitrated proteins were further confirmed by western blot with specific antibodies. Furthermore, MALDI-TOF (matrix-assisted laser desorption ionization-time of flight) analysis of protein spots, separated by two-dimensional electrophoresis from immunoprecipitated proteins, led to the identification of seven nitrated peptides corresponding to six different proteins. However, *in vivo* nitration sites among putative targets could not be identified by MS/MS. Nevertheless, an MS/MS spectrum with 3-aminoY318 instead of the expected 3-nitroY was found for cytosolic glyceraldehyde-3-phosphate dehydrogenase. Reduction of nitroY to aminoY during MS-based proteomic analysis together with the *in vivo* low abundance of these modifications made the identification of nitration sites difficult. In turn, *in vitro* nitration of methionine synthase, which was also found in the shotgun proteomic screening, allowed unequivocal identification of a nitration site at Y287.

Key words: AminoY, *Arabidopsis*, nitric oxide, nitrotyrosine, nitroY, post-translational modification, protein nitration.

Introduction

During the last 20 years, nitric oxide (NO) has been characterized as an essential regulator of many physiological processes in animals. More recently, NO has been characterized as a signal molecule regulating plant defence against pathogens (Romero-Puertas *et al.*, 2004; Mur *et al.*, 2006), resistance to abiotic stress (Zhang *et al.*, 2006), and different developmental processes including seed dormancy and germination (Bethke *et al.*, 2006; Liu *et al.*, 2007), floral transition (He *et al.*, 2004; Simpson, 2005), and leaf senescence (Mishina *et al.*, 2007). NO acts as a regulator of gene expression at the transcriptional level by regulating disease resistance processes (Polverari *et al.*, 2003) and the expression of stress-related transcription factors and signalling-related kinases (Parani *et al.* 2004), and by the interaction with other signalling mole-cules such as salicylic acid and jasmonic acid (Grün *et al.*, 2006).

Some of the regulatory properties of NO are exerted through NO-mediated post-translational modifications including nitrosylation of thiol groups and nitration of tyrosine (Y) residues (Gow *et al.*, 2004). This is thought to affect the activity, the stability, or the intracellular location of proteins, thus potentially altering their functions and eventually cell signalling. The regulation of protein function at the levels of NO-related post-translational modifications represents a new area of research in plant biology, and it will help to elucidate the mode of action of NO in regulating many processes in plants. Recent reports suggest that *S*-nitrosylation is specific and regulated (Lindermayr *et al.*, 2005; Romero-Puertas *et al.*, 2008), and it may play

a regulatory role in central processes in plants such as ethylene biosynthesis (Lindermayr *et al.*, 2006). The interaction between NO and superoxide leads to the formation of peroxynitrite, a reactive molecule with strong nitrating activity (Szabó *et al.*, 2007). The production of peroxynitrite under physiological conditions in plants has been reported (Bechtold *et al.*, 2009; Chaki *et al.*, 2009). Some proteins are targets of peroxynitrite, and the nitration of Y residues to 3-nitrotyrosine represents a hallmark of post-translational protein modification associated with human pathologies and biological ageing (Hong *et al.*, 2007). Although well characterized in mammals, scant information is available on nitration of Y residues of proteins in plants. Detection of nitrated proteins was first reported in tobacco plants with reduced nitrite reductase activity (Morot-Gaudry-Talarmain *et al.*, 2002). Later, the detection of *in vivo* nitrated proteins in plants treated with exogenous nitrating reagents (Saito *et al.*, 2006) as well as under physiological conditions in both unstressed conditions (Chaki *et al.*, 2009) and upon pathogen challenge (Romero-Puertas *et al.*, 2007; Cecconi *et al.*, 2009) was reported. However, in all these recent reports there are no data about unequivocal identification of nitrated peptides or proteins (i.e. nitration sites). Here the identification of potential *in vivo* nitration sites of some *Arabidopsis* proteins is reported. Drawbacks in proteomic approaches to identify Y nitration post-translational modification under physiological conditions are also discussed. The analysis of the regulatory functions of Y nitration of proteins in any plant biological process will require, after initial identification of potential targets, a case-by-case analysis. Recent proteomic approaches based on the protection of the primary amino group by acetylation followed by the reduction of nitroY to aminoY residues, and further derivatization of the amino group from aminoY residues (Chiapetta *et al.*, 2009; Tsumoto *et al.*, 2010), will help to overcome some of the difficulties found due to the low abundance and limited stability of nitroY residues in proteins determined to be potentially nitrated *in vivo* in this work.

Materials and methods

Plant growth conditions

Seeds of the Col-0 wild-type accession of *Arabidopsis thaliana* were sown in moistened soil and grown under photoperiodic conditions (cycles of 8 h day and 16 h night for short days, at 22 °C and 20 °C, respectively) as mentioned in different experiments. Plants were illuminated with 150 µE m^{-2} s^{-1} cool white fluorescent lamps and grown under 60% relative humidity. Alternatively, surface-sterilized seeds were germinated and grown in sterile liquid or agar-supplemented Murashige and Skoog (MS) medium (Duchefa, Haarlem, The Netherlands) with 1% (w/v) sucrose.

Protein extraction and immunoprecipitation

Two-week-old seedlings were frozen and ground in liquid nitrogen. Proteins were extracted by adding extraction buffer [10 mM TRIS-HCl, pH 7.4, 150 mM NaCl, 1% (v/v) protease inhibitor cocktail from Sigma, USA] and briefly vortexing. Protein extracts were obtained by centrifugation at 13 000 *g* at 4 °C. Protein extracts

(4× 1 mg) were pre-cleared with 50 µl of protein A–agarose (EZView Sigma, USA) for 8 h at 4 °C. The unbound fractions were each incubated overnight with 0.1 µg of monoclonal anti-3-nitroY antibody (Cayman, USA) at 4 °C. To recover 3-nitroY-containing proteins, 60 µl of protein A–agarose were added and incubated for 8 h at 4 °C. After extensive washing with extraction buffer, proteins were eluted at 95 °C with elution buffer [1% SDS, 100 mM dithiothreitol (DTT), 50 mM TRIS-HCl pH 7.6] three times. After removing agarose beads with a 0.2 µm filter (Costar Corning, NY, USA), the proteins were precipitated, combined, and processed with a 2D-Clean Up Kit (GE, UK) for subsequent two-dimensional electrophoresis (2-DE) and liquid chromatography–tandem mass spectrometry (LC-MS/MS) analysis.

2-DE and image analysis

Protein samples (100 µg) were dissolved in DeStreak Rehydration solution (GE, UK) before electrophoresis. For the first dimension, 18 cm pH 3–10 NL (non-linear) strips were passively rehydrated overnight at room temperature. The set-up of the IPGphor3 (GE, UK) was 1 h at 50 V step-and-hold, 1 h at a 150 V gradient, 1 h 30 min at a 500 V gradient, 1 h 30 min at a 1000 V gradient, 2 h at a 4000 V gradient, 2 h at a 8000 V gradient, and 7 h at a 8000 V step-and-hold. The strips were then treated with 1 mg ml^{-1} DTT for 15 min and alkylated with 25 mg ml^{-1} iodoacetamide for 15 min in equilibration buffer (6 M urea, 75 mM TRIS-HCl pH 8.8, 29.3% glycerol, 2% SDS, and 0.002% bromophenol blue), and the focused proteins were then separated on 12.5% acrylamide gels in the EttanDalt six electrophoresis unit (GE, UK) as recommended by the manufacturers for an overnight run. The gels were stained with a DeepPurple (GE, UK) or PlusOne™ Silver Staining Kit (GE, UK), digitalized with Typhoon (GE, UK), and analysed by using Image Master Platinum 5.0 (GE, UK) software.

MS analysis

Samples were digested with sequencing grade trypsin (Promega, USA). Peptide separation by LC-MS/MS was performed using an Ultimate nano-LC system (LC Packings) and a QSTAR XL Q-TOF hybrid mass spectrometer (MDS Sciex-Applied Biosystems). Samples (5 µl) were delivered to the system using a FAMOS autosampler (LC Packings) at 40 µl min^{-1}, and the peptides were trapped on a PepMap C18 pre-column (5 mm, i.d. 300 m; LC Packings). Peptides were then eluted from a PepMap C18 analytical column (15 cm, i.d. 75 m; LC Packings) at 200 nl min^{-1} and separated using a 55 min gradient of 15–50% acetonitrile (120 min for the mixtures). The QSTAR XL was operated in information-dependent acquisition mode, in which a 1 s time of flight (TOF) MS scan from 400 *m/z* to 2000 *m/z*, was performed, followed by 3 s product ion scans from 65 *m/z* to 2000 *m/z* on the three most intense doubly or triply charged ions. A database search on Swiss-Prot and NCBInr databases was performed using the MASCOT search engine (Matrix-Science). Searches were done with tryptic specificity allowing one missed cleavage and a tolerance on the mass measurement of 100 ppm in MS mode and 0.8 Da for MS/MS ions. Carbamidomethylation of C was used as a fixed modification, and oxidation of M, deamidation of D and E, and nitration or amination of Y as variable modifications.

Western blot

Protein extracts (10 µg) were separated by SDS–PAGE, blotted onto a nitrocellulose membrane, stained with Ponceau-S, and probed with antibodies at the followed dilutions: monoclonal anti-3-nitroY (Cayman Chemicals) 1:1000, anti-5×His (QIAGEN) 1:8000, polyclonal anti-GAPDH (glyceraldehyde-3-phosphate dehydrogenase) 1:10 000, anti-CA (carbonic anhydrase) 1:3000, anti-PKL (PICKLE) 1:5000; anti-FBPase (fructose bisphosphatase) 1:2000, and anti-GRP (glycine-rich RNA-binding protein) 1:2500. Secondary antibody was anti-mouse or anti-rabbit, for monoclonal

or polyclonal primary antibodies, respectively, coupled to horse-radish peroxidase (GE, UK) at 1:10 000 dilution, and an ECL kit (GE, UK) was used for visualization of proteins.

GAPDH activity

Proteins were extracted in 50 mM TRIS-HCl pH 7.4 and quantified. GAPDH activity of the extracts was assayed according to Muñoz-Bertomeu *et al.* (2009) with minor modifications. Briefly, 50 μg of protein extracts from plants treated or not with 2 mM SIN-1 (3-morpholinosydnonimine) were incubated in reaction buffer (10 mM TRIS-HCl pH 7.4, 20 mM arsenate, 2 mM NAD, 0.5 mM DTT) and the reaction was initiated by the addition of 2 mM DL-GAPDH in a final volume of 1 ml. GAPDH activity was measured following the conversion of NAD to NADH at 340 nm during 4 min.

Synthesis, purification, and nitration of His-tagged methionine synthase AtMS1

A plasmid containing *AtMS1* cDNA fused to a 6×His tag (Dixon *et al.*, 2005) was used to transform BL21(DE3) competent cells (Sigma-Aldrich) for recombinant protein production. For protein induction, cell cultures with OD=0.7 were treated with 1 mM isopropyl-β-D-1-thiogalactopyranoside (IPTG) for 5 h. Recombinant protein production was checked by SDS–PAGE and western blot analysis. Recombinant protein purification was carried out with the QIAexpress Ni-NTA Fast Start Kit (Qiagen) following the manufacturer's recommendations. Purified AtMS1 was treated or not with a nitrating buffer as described previously (Chen *et al.*, 2008). Briefly, 10 μl of purified protein was incubated with 500 μM H_2O_2 and 500 μM $NaNO_2$ in 0.1 M potassium phosphate buffer pH 7.2 for NO_2 radical-mediated protein nitration at 37 °C in the dark for 2 h in a total volume of 500 μl. To clean nitrated protein, the nitrating reaction volume was filtered trough a 10 kDa cut-off filter (Microcon, Ambion). Proteins were then analysed by SDS–PAGE and western blot. Protein nitration was confirmed with anti-3nitroY antibody (Cayman) and the anti-5×His antibody supplied by the manufacturers (QIAGEN). A duplicate gel was run and stained with Coomassie blue, and the bands were excised, trypsin digested, and further analysed by LC-MS/MS as described above.

Protein modelling and structural analysis

Three-dimensional (3-D) protein models were generated by homology modelling at the SWISS-MODEL workspace (Arnold *et al.*, 2006) using the coordinates of GAPDH from rat (PDB code 2VYN), serine hydroxymethyltransferase from *Mycobacterium tuberculosis* (PDB code 3H7F), transketolase from maize (PDB code 1ITZ), Rubisco from spinach (PDB code 1IR1), and mannitol dehydrogenase from *Cladosporium harbarum* (PDB code 3GDF) as templates. For methionine synthase, the crystal structure from *A. thaliana* was used (PDB code 1U1J). Model qualities were evaluated by ANOLEA, Verify3D, and Procheck (Melo and Feytmans, 1998; Bowie *et al.*, 1991; Laskowski *et al.*, 1996, respectively). 3-D models were visualized and manipulated with Yasara (www.yasara.org) or PyMol (www.pymol.org). The distance between residues in Amstrongs (Å) and the presence of hydrogen bonds were analysed with both programs using default settings.

Results

Crude protein extracts from *A. thaliana* plants contained a number of proteins spanning the whole range of molecular weights that cross-react with antibodies against 3-nitroY in western blot analysis (Fig. 1A). The specific cross-reaction of antibodies with 3-nitroY residues of those target proteins was checked by on-membrane protein reduction of 3-nitroY to 3-aminoY with sodium dithionite, as previously reported (Miyagi *et al.*, 2002), thus resulting in no cross-reaction with the specific antibodies (Fig. 1A). Upon antibody validation, anti-3-nitroY antibodies were used as a specific immunoprecipitation reagent together with protein A–agarose to pull-down 3-nitroY-containing proteins from crude *Arabidopsis* seedling extracts. Figure 1B shows that a small number of proteins present in the crude extracts, <20 bands as detected by Coomassie staining, were recovered in the immunoprecipitated fraction. Those proteins were further checked for cross-reaction in western blots with anti-3-nitroY antibodies (Fig. 1B). A moderate enrichment in nitrated proteins was thus observed in the immunoprecipitated fraction (Fig. 1B). Considering the low resolution capacity of one-dimensional SDS–PAGE, the complexity of the immunopurified samples was further assessed by 2-DE and the more sensitive silver staining, resulting in the separation of ∼450 spots with isoelectric points in the 3–10 range (Fig. 1C).

To identify potential *in vivo* targets of Y nitration in *Arabidopsis*, the immunopurified fraction was then analysed by MS following two different strategies. First, a shotgun analysis, based on LC-MS/MS of the immunoprecipitated proteins, was performed. Comparison of MS-generated data with the SwissProt database by specifying taxonomy for *Arabidopsis* allowed identification of 127 proteins with a statistically significant MASCOT score of at least 35 and more than two matched peptides (Table 1). Among identified proteins, 35% have homologue counterparts that have been previously reported as nitrated in non-plant organisms (Supplementary Table S1 available at *JXB* online), thus supporting the usefulness of the immunoprecipitation approach to enrich the purified fractions in *Arabidopsis* potential nitrated proteins. To validate the proteomic identification further, several of the identified proteins were detected by western blots with specific antibodies in the samples immunopurifed by precipitation with anti-3-nitroY antibodies. Some proteins identified with a MASCOT score >200, such as chloroplastic GAPDH, CA, or FBPase, and some others with a lower score such as GRP7 (score 66) and the CHD3-type chromatin remodelling factor PKL (score 58) were selected. All of them cross-reacted with proteins in the 3-nitroY-immunoprecipitated samples (Fig. 2), making the proteomic identification reliable. For proteins such as GAPDH or PKL showing no signal in the supernatant, most of the corresponding proteins were associated with IP resin and a significant proportion further recovered after washing in the IP. In contrast, the immunoprecipitation is far less efficient for others proteins such as FBPase or CA which show a similar amount of protein in the supernatant and crude extract, thus suggesting that the corresponding nitrated forms would not be abundant in the total protein population of crude extracts. Most of the proteins tested gave complex patterns of cross-reacting bands in both crude extracts and immunopurified samples (Fig. 2, Supplementary Fig. S5 at
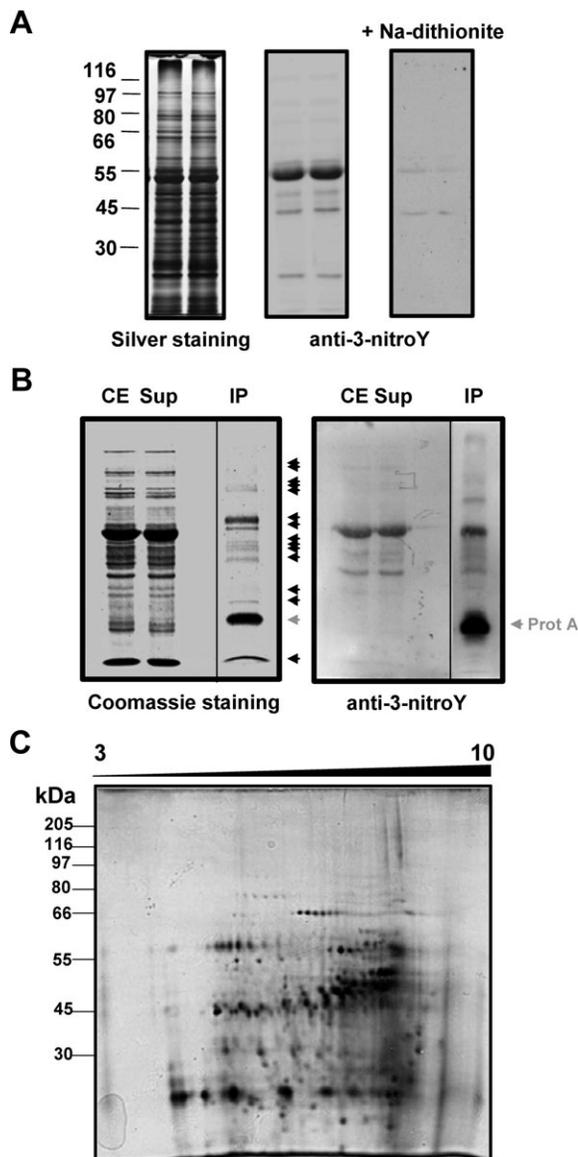
Fig. 1. Detection of 3-nitroY-containing proteins. (A) Crude protein extracts (10 µg per lane) were separated using 10% SDS–PAGE in duplicate. The left panel shows the silver-stained gel with the position of a molecular weight protein ladder. The central panel shows the corresponding western blot performed with anti-3-nitroY primary antibody, and the right panel the corresponding western blot after reduction of 3-nitroY to 3-aminoY with 100 mM sodium dithionite for 30 min. (B) *In vivo* immunoprecipitation of *Arabidopsis* 3-nitroY-containing proteins. Crude extracts (CE) were immunoprecipitated with antibody against 3-nitroY. The resulting supernatants (Sup) and immunoprecipitated proteins (IP) alongside the CE were separated by one-dimensional SDS–PAGE in duplicate and either Coomassie stained (left panel) or transferred to a nitrocellulose membrane and probed with anti-3-nitroY antibodies by western blot (right panel). Immunoprecipitated proteins detected by one-dimensional SDS–PAGE are marked with black arrowheads. The protein A which is released from the resin in the immunoprecipitates is marked with a grey arrowhead. (C) Immunoprecipitated proteins (0.1 mg) were separated by 2-DE with isoelectric focusing in the range of pH 3–10 NL and a second

dimension 10% gel. The identification of spots corresponding to nitrated proteins was performed by comparing four independent sets of 2-DE gels corresponding to biologically independent replicates with similar spot patterns. Molecular mass marker positions are indicated in kDa on the left side. Proteins were silver stained.

JXB online). This is probably due to different cross-reactive isoforms that are the result of potential post-translational modifications or to unspecific cross-reaction of the antibody.

Despite the success in identifying a large number of potentially nitrated proteins, no MS/MS spectrum with a good enough MASCOT score was obtained for nitrated peptides, thus preventing the identification of unequivocal nitration sites. To overcome this, and because the amount of protein required for the identification of nitrated peptides is often a limitation in the method, the most abundant proteins in 2-DE gels from 3-nitroY-immunoprecipitated proteins were excised from the gels, digested with trypsin, and further analysed by MALDI-TOF (matrix-assisted laser desorption ionization-time of flight). Supplementary Table S2 at *JXB* online summarizes the identified proteins, their MASCOT scores, the number of non-redundant peptides, and the corresponding sequence coverage. Twenty-two proteins were identified with a MASCOT score >59, considered as significant in the proteomic analysis. Unfortunately, no MS/MS spectra with a high enough score corresponding to a *bona fide* Y-nitrated peptide could be obtained. However, six out of 22 identified proteins showed MALDI-TOF spectra for potentially nitrated peptides with a signal/noise ratio >25, considered as significant in the analysis. The simultaneous identification of nitrated peptides and their unmodified forms in addition to the length of the nitrated peptides identified (≥7 amino acid residues) makes the identification more reliable (Stevens *et al.*, 2008). Table 2 shows the identity of those proteins and the corresponding nitrated peptides with the signal/noise ratio, the molecular mass of the unmodified and modified peptides, and the corresponding +45 shift to the modification of Y to nitroY. Three out of those six proteins (Rubisco, Rubisco activase, and transketolase) showed nitrated peptides containing a single Y residue and a +45 mass shift, thus allowing the assignment of a putative nitration site for those proteins. For serine hydroxymethyltransferase, the nitrated peptide contained two Y residues and showed a mass shift of +90, compatible with two Y nitration sites. Finally, for the other two proteins, a cytosolic GAPDH and a putative mannitol dehydrogenase, the nitrated peptides contained two Y residues and showed a mass shift of +45, corresponding to a single nitration event, so no nitration site could be proposed for these proteins (Table 2).

Y residues contained in the nitrated peptides were checked to see if they fulfilled the previously characterized factors determining the selectivity of Y nitration in proteins. These factors include the proximity of a basic amino acid within the primary sequence, the exposure of the aromatic

Table 1. Immunopurified Y-nitrated proteins identified in Arabidopsis thaliana seedlings by a shotgun LC-MS/MS approach

Those proteins that have been previously reported as nitrated in other plant systems are been marked with a single (Chaki *et al.*, 2009) or double asterisk (Cecconi *et al.*, 2009).

SwissProt locus	AGI code	Description	MASCOT score	Peptides matched (no.)	Best two peptides (ion score)
ATPB_ARATH	AtCg00480	ATP synthase subunit beta	1150	23	R.FVQAGSEVSALLGR.M (85) K.IGLFGGAGVGK.T (80)
METE_ARATH	At5g17920	Methionine synthase 1	1014	27	K.DEALFSANAAALASR.R (97) K.MLAVLEQNILWVNPDCGLK.T(91)
G3PB_ARATH	At1g42970	GAPDH B, chloroplast	884	22	K.IVDNETISVDGK.L (85) R.KDSPLEVVVLNDSGGVK.N (75)
G3PA_ARATH	At3g26650	GAPDH A, chloroplast	831	18	R.VPTPNVSVVDLVVQVSK.K (68) K.KVIITAPGK.G (60)
RCA_ARATH	At2g39730	Rubisco activase, chloroplast**	761	20	R.GLAYDTSDDQQDITR.G (81) R.VQLAETYLSQAALGDANADAIGR.G (72)
GOX1_ARATH	At3g14415	Probable peroxisomal glycolate oxidase1	670	16	R.AASAAGTIMTLSSWATSSVEEV ASTGPGIR.F (101) K.DIQWLQTITNMPILVK.G (58)
GOX2_ARATH	At3g14420	Probable peroxisomal glycolate oxidase2	651	16	R.AASAAGTIMTLSSWATSSV EEVASTGPGIR.F (101) R.IPVFLDGGVR.R (52)
SAHH1_ARATH	At4g13940	Adenosyl homocysteinase 1*	581	18	K.VALLHLGK.L (55) R.DSAAVFAWK.G (54)
PGKH_ARATH	At1g56190	Phosphoglycerate kinase, chloroplast	542	14	K.LASLADLYVNDAFGTAHR.A (77) K.FAAGTEAIANK.L (75)
ATPA_ARATH	AtCg00120	ATP synthase subunit alpha**	504	12	R.EAYPGDVFYLHSR.L (64) R.EQHTLIIYDDLSK.Q (62)
EFTU_ARATH	At4g20360	Elongation factor Tu, chloroplast	491	13	K.KYDEIDAAPEER.A (72) R.SYTVTGVEMFQK.I (54)
G3PC_ARATH	At3g04120	GAPDH C, cytosolic	479	13	R.VPTVDVSVVDLTVR.L (71) K.KVVISAPSK.D (52)
CAHC_ARATH	At3g01500	Carbonic anhydrase 1, chloroplast	475	13	K.YGGVGAAIEYAVLHLK.V (64) R.EAVNVSLANLLTYPFVR.E (60)
EF1A_ARATH	At1g07940	Elongation factor 1-alpha	450	11	R.EHALLAFTLGVK.Q (103) K.FHINIVVIGHVDSGK.S (82)
ACT7_ARATH	At5g09810	Actin-7	448	12	K.SEYDESGPSIVHR.K (75) K.NYELPDGQVITIGAER.F (57)
ACT2_ARATH	At3g18780	Actin-2	430	12	K.NYELPDGQVITIGAER.F (57) K.AGFAGDDAPR.A (52)
KPPR_ARATH	At1g32060	Phosphoribulokinase, chloroplast	418	13	R.LDELIYVESHLSNLSTK.F (55) K.ILVIEGLHPMFDER.V (52)
RUBB_ARATH	At1g55490	Rubisco large subunit beta	389	13	R.GYISPYFVTDSEK.M (71) K.YEDLMAAGIIDPTK.V (52)
CAH2_ARATH	At5g14740	Carbonic anhydrase 2	379	11	R.EAVNVSLANLLTYPFVR.E (60) K.VENIVVIGHSACGGIK.G (59)
TBA6_ARATH	At4g14960	Tubulin alpha-6 chain	358	11	R.AVFVDLEPTVIDEVR.T (67) R.LVSQVISSLTASLR.F (50)
METK1_ARATH	At1g02500	*S*-Adenosyl methionine synthetase 1	334	11	R.FVIGGPHGDAGLTGR.K (73) K.IIIDTYGGWGAHGGGAFSGK.D (64)
RUBA_ARATH	At2g28000	Rubisco large subunit alpha, chloroplast	331	11	K.VVNDGVTIAR.A (60) K.TNDSAGDGTTTASILAR.E (56)
METK2_ARATH	At4g01850	*S*-Adenosyl methionine synthetase 2	326	11	R.FVIGGPHGDAGLTGR.K (73) K.IIIDTYGGWGAHGGGAFSGK.D (64)
GLNA2_ARATH	At5g35630	Glutamine synthetase, chloroplast/mitochondrial**	314	10	K.VSGEVPWFGIEQEYTLLQQNVK.W (76) K.HETASIDQFSWGVANR.G (42)
SGAT_ARATH	At2g13360	Serine-glyoxylate aminotransferase	306	10	R.AALDLIFEEGLENIIAR.H (61) K.VFFDWNDYLK.F (42)
RBS1A_ARATH	At1g67090	Rubisco small subunit 1A, chloroplast	299	9	K.LPLFGCTDSAQVLK.E (71)

Table 1. *Continued*

SwissProt locus	AGI code	Description	MASCOT score	Peptides matched (no.)	Best two peptides (ion score)
TBA3_ARATH	At5g19770	Tubulin alpha-3/alpha-5 chain	284	8	K.EVDYLIR.N (46) R.AVFVDLEPTVIDEVR.T (67)
PORB_ARATH	At4g27440	Protochlorophyllide reductase B	263	12	R.LISQIISSLTTSLR.F (65) R.LLLDDLKK.S (53)
RBS1B_ARATH	At5g38430	Rubisco small subunit 1B, chloroplast	254	7	K.GYVSETESGKR.L (46) K.LPLFGCTDSAQVLK.E (71)
ILV5_ARATH	At3g58610	Ketol-acid reductoisomerase, chloroplast	240	9	K.EVDYLLR.N (46) K.VSLAGYEEYIVR.G (44)
TBB4_ARATH	At5g44340	Tubulin beta-4 chain	226	8	K.APVSLDFETSVFK.K (43) K.LAVNLIPFPR.L (54)
HSP71_ARATH	At5g02500	Heat shock cognate 70 kDa protein 1*	217	10	R.YLTASAVFR.G (35) R.MVNHFVQEFK.R (40)
F16P1_ARATH	At3g54050	Fructose-1,6-bisphosphatase	214	10	K.ATAGDTHLGGEDFDNR.M (35) R.TLLYGGIYGYPR.D (58)
TBB2_ARATH	At5g62690	Tubulin beta-2/beta-3 chain	203	9	R.VLDIQPTEIHQR.V (42) K.LAVNLIPFPR.L (54)
TBB1_ARATH	At1g75780	Tubulin beta-1 chain	193	8	R.AVLMDLEPGTMDSLR.S (35) K.LAVNLIPFPR.L (54)
PGMP_ARATH	At5g51820	Phosphoglucomutase, chloroplast	173	9	R.AVLMDLEPGTMDSIR.S (35) K.SLPTKPIEGQK.T (30)
P2SAF_ARATH	At5g23120	Photosystem II stability/assembly factor HCF136	172	8	K.LPFFEVPTGWK.F (26) R.ADGGLWLLVR.G (40)
HSP73_ARATH	At3g09440	Heat shock cognate 70 kDa protein 3*	172	7	K.GTGITEEFEEVPVQSR.G (34) R.MVNHFVQEFK.R (40)
APX1_ARATH	At1g07890	L-Ascorbate peroxidase 1, cytosolic	161	5	K.ATAGDTHLGGEDFDNR.M (35) K.EGLLQLVSDK.A (44)
MTDH_ARATH	At4g39330	Probable mannitol dehydrogenase	139	5	K.QMGLSDKDIVALSGAHTLGR.C (35) K.NYGGYSENIVVDQR.F (47)
CD48A_ARATH	At3g09840	Cell division control protein 48 A	120	6	K.NYGGYSENIVVDQR.F (34) R.KGDLFLVR.G (29)
GME_ARATH	At5g28840	GDP-mannose 3,5-epimerase	112	5	R.IVSQLLTLMDGLK.S (29) R.SFTFIDECVEGVLR.L (43)
GBLP_ARATH	At1g18080	Guanine nucleotide-binding protein subunit beta	103	4	K.KLPIHHIPGPEGVR.G (31) R.LWDLAAGVSTR.R (42)
CLPP_ARATH	AtCg00670	ATP-dependent Clp protease	99	2	K.DGVVLLWDLAEGK.K (27) R.SPGEGDTSWVDIYNR.L (70)
GCST_ARATH	At1g11860	Aminomethyltransferase, mitochondrial	99	5	R.TGKPIWVISEDMER.D (30) K.GGDVSWHIHDER.S (25)
AAT5_ARATH	At4g31990	Aspartate aminotransferase, chloroplast	98	5	R.AEGGFLGADVILQQLK.D (24) K.ATAELLFGAGHPVIK.E (27)
ACA9_ARATH	At3g21180	Ca-transporting ATPase 9, plasma membrane	98	7	R.VATIQGLSGTGSLR.L (24) R.VAIDSMAK.N (28)
RH56_ARATH	At5g11200	DEAD-box ATP-dependent RNA helicase 56	97	5	R.QAALVLNASRR.F (21) K.LSEMEKNR.K (30)
ENO_ARATH	At2g36530	Enolase	96	6	K.VSVFYGGVNIK.I (25) K.AGAVVSGIPLYK.H (30)
MRP7_ARATH	At3g13100	Multidrug resistance-associated protein 7	86	7	K.LAMQEFMILPVGAASFK.E (30) R.YGPHLPMVLRGLTCTFR.G (20)
AFB3_ARATH	At1g12820	AUXIN SIGNALLING F-BOX 3	84	6	R.GIEAGWLK.K (17) R.LWILDSIGDK.G (23)
PDX13_ARATH	At5g01410	Pyridoxal biosynthesis protein	79	4	R.LMSCAPQLVDLGVGSYE NEPDPESFAK.L (17) K.VGLAQMLR.G (43)
PDX11_ARATH	At2g38230	Pyridoxal biosynthesis protein	75	3	R.NMDDDEVFTFAK.K (14) K.VGLAQMLR.G (43) K.IAAPYDLVVQTK.E (20)

Table 1. *Continued*

SwissProt locus	AGI code	Description	MASCOT score	Peptides matched (no.)	Best two peptides (ion score)
EFTM_ARATH	At4g02930	Elongation factor Tu, mitochondrial	75	2	R.GSALSALQGTNDEIGR.Q (49) K.LMDAVDEYIPDPVR.V (26)
MDR11_ARATH	At3g28860	Multidrug resistance protein 11 (P-glycoprotein 19)	73	6	K.SSVIAMIER.F (24) R.AVLKNPTVLLLDEATSALDAESEC VLQEALERLMR.G (22)
MDHP_ARATH	At3g47520	Malate dehydrogenase, chloroplast	70	3	K.DVNVVVIPAGVPR.K (35) K.LFGVTTLDVVR.A (22)
SR54C_ARATH	At5g03940	Signal recognition particle 54 kDa protein, chloroplast	70	5	R.GVKPDQQLVK.I (16) R.QEDAEDLQKK.I (16)
MDHG1_ARATH	At5g09660	Malate dehydrogenase, glyoxysomal	70	3	R.TGAEEVYQLGPLNEYER.I (31) K.LLGVTTLDVAR.A (30)
TAF1B_ARATH	At3g19040	Transcription initiation factor TFIID subunit 1-B	69	7	R.ENLKQLNSDARGR.L (20) K.EIGTPICQMKKILK.E (17)
TYW23_ARATH	At4g04670	tRNA wybutosine-synthesizing protein	69	5	R.ADPLNILNDVWR.L (24) K.RVIIAIRCSIR.M (15)
CATA3_ARATH	At1g20620	Catalase-3	69	3	R.LGPNYLQLPVNAPK.C (32) K.GFFEVTHDISNLTCADFLR.A (28)
KASC1_ARATH	At5g46290	3-Oxoacyl-[acyl-carrier-protein] synthase I, chloroplast	68	3	K.LLSGESGISLIDR.F (53) R.ADGLGVSSCIER.C (9)
ATPG1_ARATH	At4g04640	ATP synthase gamma chain 1, chloroplast	68	2	R.ALQESLASELAAR.M (52) R.ASSVSPLQASLRELR.D (16)
GRP7_ARATH	At2g21660	Glycine-rich RNA-binding protein 7	66	1	R.ALETAFAQYGDVIDSK.I (66)
FDH_ARATH	At5g14780	Formate dehydrogenase, mitochondrial	66	5	R.QAVVDAVESGHIGGYSGDVWD PQPAPK.D (18) R.LQMAPELEK.E (17)
HSP83_ARATH	At5g56010	Heat shock protein 81-3*	62	5	K.GIEVLYMVDAIDEYAIGQLK.E (21) K.EGQNDIFYITGESK.K (16)
TGA2_ARATH	At5g06950	Transcription factor TGA2	61	4	K.LTQLEQELQR.A (19) R.LQTLQQMIR.V (15)
TCPA_ARATH	At3g20050	T-complex protein 1 subunit alpha	61	6	R.NKIHPTSIISGYR.L (19) R.GANDYMLDEMER.A (15)
CAPP3_ARATH	At3g14940	Phosphoenolpyruvate carboxylase 3	60	4	K.LLVSEDLWAFGEKLR.A (22) K.RLVSDLGK.S (15)
WRK19_ARATH	At4g12020	WRKY transcription factor 19	60	6	K.CTYLGCPSKRK.V (19) K.LCQVEGCQKGAR.D (16)
THI4_ARATH	At5g54770	Thiazole biosynthetic enzyme, chloroplast	59	2	K.HAALFTSTIMSK.L (33) K.ALDMNTAEDAIVR.L (26)
OMT1_ARATH	At5g54160	Quercetin 3-O-methyltransferase 1	59	2	K.NPEAPVMLDR.I (34) K.VLMESWYHLK.D (25)
IF5A2_ARATH	At1g26630	Eukaryotic translation initiation factor 5A-2 (eIF-5A)	59	2	K.LPTDDGLTAQMR.L (33) K.CHFVAIDIFTAK.K (26)
PKL_ARATH	At2g25170	PICKLE chromatin-remodelling factor	58	6	K.GLLHPYQLEGLNFLR.F (19) K.AYKSNHRLK.T (14)
Y1934_ARATH	At1g09340	Uncharacterized protein chloroplast	57	3	K.SSLSAEGFDVVYDINGR.E (26) R.FIGLFLSR.I (16)
VIN3_ARATH	At5g57380	VERNALIZATION-INSENSITIVE 3	56	5	R.GIVNRLSSGVHVQKLCSQ AMEALDK.V (27) R.NEIMKIICAEMGKER.K (14)
PME4_ARATH	At2g47030	Pectinesterase-4 (VANGUARD1-like protein 1)	54	6	K.AVQGICQSTSDKASCVK.T (16) K.NTAGPMGHQAAAIRVNGDRAV IFNCR.F (12)
APT1_ARATH	At1g27450	Adenine phosphoribosyltransferase 1 (APRT 1)	54	3	R.AIIIDDLIATGGTLAAAIR.L (35) K.DTIALFVDR.Y (15)
DRL19_ARATH	At1g63350	Putative disease resistance protein At1g63350	54	4	R.NAELQRLCLCGFCSKSLTTSYR.Y (17) K.MCLLYCALFPEDAK.I (16)
FABG_ARATH	At1g24360	3-Oxoacyl-[acyl-carrier-protein] reductase, chloroplast	54	3	K.WGTIDVVVNNAGITR.D (25)

Table 1. *Continued*

SwissProt locus	AGI code	Description	MASCOT score	Peptides matched (no.)	Best two peptides (ion score)
BSL1_ARATH	At4g03080	Serine/threonine-protein phosphatase BSL1	53	4	K.ILGTIPLGR.Y (19) K.IICMHGGIGR.S (16)
PER9_ARATH	At1g44970	Peroxidase 9	52	3	R.HGAASVGIRIYVHGGLR.G (16) K.AYAEDERLFFQQFAK.S (26)
UPL1_ARATH	At1g55860	E3 ubiquitin-protein ligase UPL1	52	5	K.EPRMAASLLR.L (13) K.LLSDIVLMYSHGTSVILR.R (20)
HDA5_ARATH	At5g61060	Histone deacetylase 5	51	3	R.LIDFDNKKAYFR.S (16) R.KVGLIYDETMCK.H (24)
HAC12_ARATH	At1g16710	HAC12 histone acetyltransferase	51	5	K.LQLAGVSQR.C (18) K.LTTHPSLADQNAQNK.E (14)
MRP14_ARATH	At3g59140	Multidrug resistance-associated protein 14	50	7	K.ASGQSDFSGNASK.D (13) R.IATFLEAPELQGGERRR.K (16)
ASHH2_ARATH	At1g77300	Histone-lysine N-methyltransferase ASHH2	50	6	R.VVAVENPTKPVK.E (11) K.ILPRPRPR.M (13)
ATM_ARATH	At3g48190	Serine/threonine-protein kinase ATM (PI3Kc_related)	47	8	K.SPSENGSHLIPNAKKAK.H (13) R.RVLLQILGCEKCTMQHL LQSASLLR.K (14)
FBX10_ARATH	At1g51290	Putative F-box only protein 10	47	4	K.QIPMAQLHENEGRK.S (11) R.LVICCYDETQQVYIYIVRR.N (16)
PSBP1_ARATH	At1g06680	Oxygen-evolving enhancer protein 2-1, chloroplast	45	3	K.YVIGYDNKK.R (14) K.TNTDFLPYNGDGFK.V (25)
CHLD_ARATH	At4g18480	Magnesium-chelatase subunit chlD, chloroplast	45	3	K.EIEYPGQVLR.F (12) K.IYKAGMSLLVIDTENK.F (26)
FBK38_ARATH	At2g29800	Putative F-box/Kelch-repeat	44	3	R.VAAVGIATQFQERCNEVFR.M (22) K.MANFGGKLVILGCYR.S (20)
GLYM_ARATH	At4g37930	Serine hydroxymethyltransferase mitochondrial	44	4	R.HLRNMKR.D (16) R.GFVEEDFAK.V (22)
SCP37_ARATH	At3g52010	Serine carboxypeptidase-like 37	44	3	K.VLEAVHIASNK.N (11) K.AIHANTTK.L (19)
COL14_ARATH	At2g33500	CONSTANS-LIKE 14	44	3	K.KLPGQPSGVSFR.Q (18) K.LCLPCDQHVHSANLLSR.K (20)
SYV_ARATH	At1g14610	Valyl-tRNA synthetase	43	7	K.SNNIPAAIHSHK.S (14) K.SDLFKADAK.S (16)
DRP1D_ARATH	At2g44590	Dynamin-related protein 1D	43	3	K.INLDILRVVGYR.Q (13) R.MQCAKRLELYK.K (22)
VATB_ARATH	At1g76030	Vacuolar ATP synthase subunit B	43	3	R.MGSEYLAK.L (14) R.NIFQSLDLAWTLLR.I (16)
SIZ1_ARATH	At5g60410	E3 SUMO-protein ligase SIZ1	42	5	R.KFVMQGAYDTR.N (15) K.WQCPICLK.N (15)
HAC2_ARATH	At1g67220	HAC2 histone acetyltransferase	42	4	R.HRSLNKICIILCAGK.N (12) R.ACTGCYTKNRTLR.H (16)
TMK1_ARATH	At1g66150	Putative receptor protein kinase TMK1 precursor	42	4	K.LGTVVDIIEPMKCDER.S (11) K.GNDPCTNWIGIACSNGNI TVISLEK.M (18)
SYM_ARATH	At4g13780	Probable methionyl-tRNA synthetase	42	3	K.VVNLTNNHLQGPVPVFK.S (12) R.LVEGSCPFEGCNYDSAR.G (26)
WEE1_ARATH	At1g02970	Wee1-like protein kinase	41	3	K.CKVCQNTPR.I (12) R.AMPPPCLK.N (19)
ARR12_ARATH	At2g25180	Two-component response regulator	41	5	K.LPLLPGHSLQLQQLLK.T (15) –.MTVEQNLEALDQFPVGMR.V (17)
CESA4_ARATH	At5g44030	Cellulose synthase A catalytic subunit 4	41	4	R.HCQYHVTTTNQAQK.A (9) K.KAGAMNAMVR.V (22)
AUR2_ARATH	At2g25880	Serine/threonine-protein kinase Aurora-2	41	3	K.SSLMSQKNFEKR.F (12) R.LYGYFYDQKRVYLILEYAVR.G (18)
Y1838_ARATH	At1g18380	Uncharacterized protein At1g18380	41	3	M.LYQAASEAAQK.R (14) R.YIMEDKACR.R (32)

Table 1. *Continued*

SwissProt locus	AGI code	Description	MASCOT score	Peptides matched (no.)	Best two peptides (ion score)
2AAA_ARATH	At1g25490	Serine/threonine-protein phosphatase 2A regulatory subunit A alpha	41	4	R.SSDSDEGCMKYAEIPMLR.S (8) R.LAGGEWFAAR.V (17)
FBK84_ARATH	At4g19865	F-box/Kelch-repeat protein At4g19865	40	3	R.RAAASNLGK.F (11) K.IEFGNVNEMCAYDTKLCK.W (20)
MSH3_ARATH	At4g25540	DNA mismatch repair protein MSH3	40	4	K.IYVMGGCQGLKDEPWAEVFNTK.T (10) R.LVNAGYKIGVVK.Q (17)
DCDA1_ARATH	At3g14390	Diaminopimelate decarboxylase 1, chloroplast	39	1	R.LVNAGYK.I (13) R.DAAVLMIEYIDEIR.R (39)
GL25_ARATH	At5g26700	Probable germin-like protein subfamily 2–5	39	3	R.IDYAPNGLNPPHVHPR.A (17) K.LPGLNTLGLSMSR.I (14)
CYSK1_ARATH	At4g14880	Cysteine synthase (OAS-TL A)	39	3	K.IDGFVSGIGTGGTITGAGK.Y (21) R.IGFSMISDAEK.K (15)
MRP13_ARATH	At1g30410	Multidrug resistance-associated protein 13	39	4	R.KKYYNCVLGLLACYCVVEPVLR.L (22) R.SVLIKQEER.E (14)
ERG11_ARATH	At5g24150	Squalene monooxygenase 1,1	39	3	R.RLLQPLSNLGNAQK.I (18) R.LFGLAMKMLVPHLK.A (13)
DPOLA_ARATH	At5g67100	DNA polymerase alpha catalytic subunit	38	4	K.NGCNVLSIENSERALLNRLFL ELNK.L (14) R.KRSGILSHFTVVR.N (13)
CWP17_ARATH	At2g06850	23 kDa cell wall protein	38	3	–.IPCRKAIDVPFGTR.Y (19) R.KAIDVPFGPR.Y (13)
MOCOS_ARATH	At1g16540	Molybdenum cofactor sulphurase (ABA3)	38	7	K.LLKSLTPSAIWMHTTSLSIYVK.K (12) R.YEIDEKR.Q (10)
ALA11_ARATH	At1g13210	Phospholipid-transporting ATPase 11	38	5	K.SLTYALEDDFKK.K (18) R.SMAMRSNGSSLVGDDLDVVV DQSGPK.I (10)
TAP1_ARATH	At1g70610	Antigen peptide transporter-like 1, chloroplast	38	3	R.GCFFGIANMILVKRMR.E (16) R.QRIGYVGQEPK.L (12)
AGO1_ARATH	At1g48410	Protein argonaute	37	2	R.INLLDEEVGAGGQR.R (36) R.GYGQPPQQQQQYGGPQ EYQGRGR.G (4)
FBK19_ARATH	At1g32430	Putative F-box/Kelch-repeat protein At1g32430	37	2	K.VEVRELTLNNPGLK.A (22) R.CIKLEVNEPSLDFLGIGYDNNK.R (14)
LUMI_ARATH	At4g02560	LUMINIDEPENDENS	37	2	K.KHMLGSNPSYNK.E (21) K.HDSSTHPYWNQNK.R (18)
CAPP1_ARATH	At1g53310	Phosphoenolpyruvate carboxylase 1	36	2	K.LEELGSVLTSLDPGDSIVIAK.A (23) K.GIAAGLQNTG.– (14)
WBC16_ARATH	At3g55090	Probable white–brown complex homologue protein 16	36	2	K.TIIGDEGHR.G (29) R.ILFYLCLLLGSKNK.R (8)
CNGC4_ARATH	At5g54250	Cyclic nucleotide-gated ion channel 4	36	3	R.IGLTCGGR.R (36) R.GVDECEMVQNLPEGLR.R (5)
U496I_ARATH	At2g18630	UPF0496 protein At2g18630	36	2	K.INSEYTEHLSSYER.A (21) K.YEKVVRGQK.E (13)
ARFM_ARATH	At1g34170	Auxin response factor 13	36	2	K.FVDAMNNNYIVGSR.F (20) K.FVDAMNNNYIVGSRFR.M (16)
CYSKM_ARATH	At3g59760	Cysteine synthase, mitochondrial (OAS-TL C)	35	3	K.IQGIGAGFIPK.N (15) R.IGYSMVTDAEQKGFISPGK.S (15)

ring to the surface of the protein, the location of the Y residue on a loop structure, its association with a neighbouring negative charge, and the proximity of the proteins to the site of generation of nitrating agents (Souza *et al.*, 1999; Ischiropoulos, 2003; Chaki *et al.*, 2009). With the exception of Rubisco activase, for which no structural model is available, the structures of the proteins were modelled as indicated in the Materials and methods. All putative nitrated Y residues had acidic residues close enough (<10 Å from the Y target) and all of them have basic amino acids in the primary sequence flanking the Y residue (Table 3). However, only Y337 and Y135 from transketolase and putative mannitol dehydrogenase, respectively, were located in loops, and most of them showed accessibile solvent area

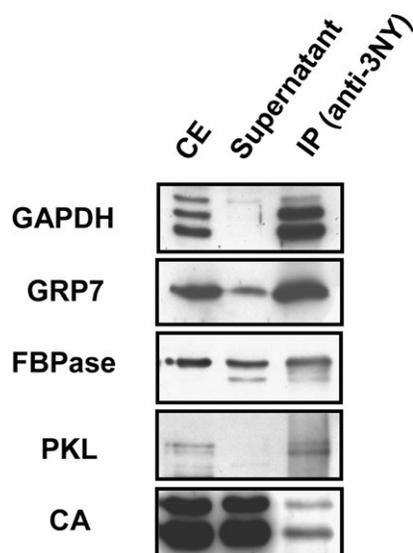(ASA) indexes <70 (Table 3), thus having a low probability of being efficiently exposed to the solvent. Regarding the

Fig. 2 Confirmation of the presence of proteins identified through shotgun proteomic analysis in the immnunopurified nitroproteome. Crude protein extracts (CE) were immunoprecipitated with anti-3-nitroY (anti-3-NY) antibodies. The CE, supernatant, and immuno-precipitate (IP) were separated by 12% SDS–PAGE, transferred to a nitrocellulose membrane, and probed with specific antibodies raised against chloroplastic glyceraldehyde-3-phosphate dehydrogenase (GAPDH), glycine-rich protein 7 (GRP7), fructose bisphosphatase (FBPase), PICKEL (PKL), or carbonic anhydrase (CA). The procedure started from 1mg of total protein in the crude extract that was immunoprecipitated as described in the Materials and methods, and then the whole IP was loaded on the gel along with 1% of the CE input and the corresponding supernatant.

proximity of the proteins to the site of generation of nitrating agents, all the proteins identified are located in subcellular compartments previously characterized as sites of NO and superoxide production in plants, such as apoplasts, mitochondria, and chloroplasts (Corpas *et al.*, 2001; Bethke *et al.*, 2004; Gupta *et al.*, 2005; Jasid *et al.*, 2006; Flores-Pérez *et al.*, 2008; Igamberdiev and Hill, 2009). In addition, the fact that some of the Y residues found to be potentially nitrated are highly conserved Y residues in proteins functionally homologous in other organisms (Supplementary Fig. S1 at *JXB* online) confers potential functional relevance to this post-translational modification as a regulatory mechanism of their activity/function. Regarding this, it has been confirmed that treatment of seedlings with a peroxynitrite donor, such as SIN-1, led to inhibition of GAPDH activity (Fig. 3A).

Despite efforts made to identify sites of *in vivo* Y nitration among proteins immunoprecipitated with anti-3-nitroY, not a single MS/MS spectrum corresponding to a nitrated peptide was identified. There might be two explanations for this lack of success. First, the nitrated form of the identified proteins could be naturally very low abundant in the analysed samples, thus making MS/MS-based identification extremely difficult. Secondly, the lack of detection of nitrated peptides may be the result of the unstable nature of nitroY under the conditions used to process samples by MS. Regarding the latter, it has been proposed that the nitro group linked to Y residues of proteins can be reduced to an amino group (Sarver *et al.*, 2001; Tsumoto *et al.*, 2010). When crude proteomic data from spots excised from gels after 2-DE were searched for aminoY instead of nitroY post-translational modification, an MS/MS fragmentation spectrum corresponding to LVSWYDNEWGYSSR peptide (monoisotopic mass of neutral peptide of 1776.7631; ion

Table 2. Putative Y-nitrated peptides identified by MALDI-TOF from 2D gel-excised spots

Samples containing 3-nitroY immunopurified proteins were separated by 2-DE and identified by MALDI-TOF as described in the Materials and methods. The AGI identifiers for each identified protein are included along with the corresponding Y-nitrated peptide sequence (the residues susceptible to Y nitration are underlined and unequivocal nitration of Y is indicated in bold). Error (difference between the experimental and calculated masses); signal-to-noise ratio, relative molecular mass (M_r) observed for the modified and the corresponding unmodified peptide that appeared in the same MASCOT search. Values in parentheses indicate the absence of the unmodified peptide. The mass shift (Shift) and the modifications of the corresponding peptide with their respective mass increases are also shown. Those proteins that have been previously reported as nitrated in other plant systems have been marked with a single (Chaki *et al.*, 2009) or double asterisk (Cecconi *et al.*. 2009).

Description	AGI identifier	Peptide sequence	Error	Signal-to-noise	M_r (observed) (unmodified)	M_r (observed)	Shift	Modification
Rubisco activase, chloroplast precursor	At2g39730	351R.V**Y**DDEVR.K359	0.01	110	895.34	940.41	+45.07	NitroY (+45)
		72R.GLA**Y**DTSDDQQDITR.G88	−0.05	25	1697.66	1744.66	+46.97	2 Deamination (+2) NitroY (+45)
Serine hydroxymethyl transferase	At4g13930	160K.VNFTTG**Y**ID**Y**DKLEEK.A177	0.03	60	1934.83	2025.92	+91.09	Deamination (+1) 2 NitroY (+90)
Transketolase, putative*	At3g60750	333K.ANS**Y**SVHGAALG EKEVEATR.N354	0.15	57	(2090.15)	2135.15	(+45)	NitroY (+45)
Glyceraldehyde-3-phosphate dehydrogenase, cytosolic	At3g04120	313K.LVSW**Y**DNEWG**Y**SSR.V328	−0.06	50	1761.72	1806.72	+45	NitroY (+45)
Probable mannitol dehydrogenase	At4g39330	133K.N**Y**GG**Y**SENIVVDQR.F148	−0.04	27	1613.63	1658.70	+45.07	NitroY (+45)
Rubisco large chain precursor**	AtCg00490	236K.GH**Y**LNATAGTCEEMIK.R253	0.04	25	(1794.84)	1839.84	(+45)	NitroY (+45)

Table 3. Structural features of potential Y targets of nitration in MALDI-TOF-identified proteins

Protein annotation and AGI code along with the Putative nitrated Y are indicated. Parameters were calculated as described in the Materials and methods. Accessible solvent area (ASA) was calculated by NetSurfP software (Petersen *et al.* 2009).

Protein/AGI	Putative nitrated Y	Distance to D/E	Proximal basic amino acids in primary sequence	Location in loop	ASA
Rubisco activase, chloroplast precursor_ At2g39730	Y353	(No model)	R351, R358, K359	(No model)	5.45
	Y76		R72		79.13
Serine hydroxymethyl transferase_ At4g13930	Y167	5.99 Å to E342	K160, K172, K176	No	62.38
	Y170	5.04 Å to D197	K160, K172, K176	No	23.35
Transketolase, putative_ At3g60750	Y337	9.01 Å to D268	K333, H340, K347	Yes	66.16
Glyceraldehyde-3-phosphate dehydrogenase, cytosolic_ At3g04120	Y318	6.08 Å to D319	K313, R327	No	7.35
	Y324	6.61 Å to E321	K313, R327	No	19.17
Probable mannitol dehydrogenase_ At4g39330	Y135	4.31 Å to E8	K133, R147	Yes	34.66
	Y138	3.75 Å to D53	K133, R147	No	13.55
Rubisco large subunit precursor_ AtCg00490	Y239	6.33 Å to E158	K236, H238, K252, R253	No	6.37

score 43; expected 0.00088) was found for cytosolic GADPH (G3PC). This spectrum included a +15 shift compatible with an amino modification of Y318 (Fig. 3B). These data suggest that from two Y residues found as potential nitration targets in G3PC (Table 2), part of the 3-nitroY318 residues in the protein population might undergo reduction to 3-aminoY318 under the conditions used for MS analysis. Since reduction may occur with any nitroY, the crude data from LC-MS/MS shotgun analysis were searched for aminoY modification, and 51 putative aminoY-containing peptides with ion scores >15 were found that corresponded to 47 different proteins (Supplementary Table S3 at *JXB* online). Comparison of nitroY and aminoY searches led to only five peptides that were detected to be Y nitrated or aminated in the same residue, but all of them had ion scores <10, thus suggesting that the partial reduction of nitroY may lower the abundance of both modifications, making MS identification even more difficult.

To overcome the low abundance of nitrated forms of proteins found *in vivo*, one of the proteins identified in the screen as potentially nitrated, 5-methyl tetrahydropteroyl-triglutamate-homocysteine *S*-methyltransferase or methionine synthase 1 (AtMS1) was expressed as a 6×His-tagged version in bacteria. The tagged recombinant protein was expressed to moderately high levels by 5 h after induction with IPTG (data not shown). Crude recombinant extracts were checked for AtMS1 protein content by western blot with anti-5×His tag antibodies and subsequently purified with Ni-resin. The purified protein was then split into two equivalent samples, one of them being nitrated *in vitro* whereas the other was used as control of no exogenous nitration. The efficiency of nitration was then checked by western blot with anti-3-nitroY. No cross-reacting band was detected in the control protein but a strong signal was observed in the nitrated recombinant AtMS1 protein (Fig. 4A). Both samples had comparable levels of recombinant protein as confirmed by western blot with anti-5×His antibodies (Fig. 4A). A duplicate one-dimensional SDS–polyacrylamide gel was stained with Coomassie blue and
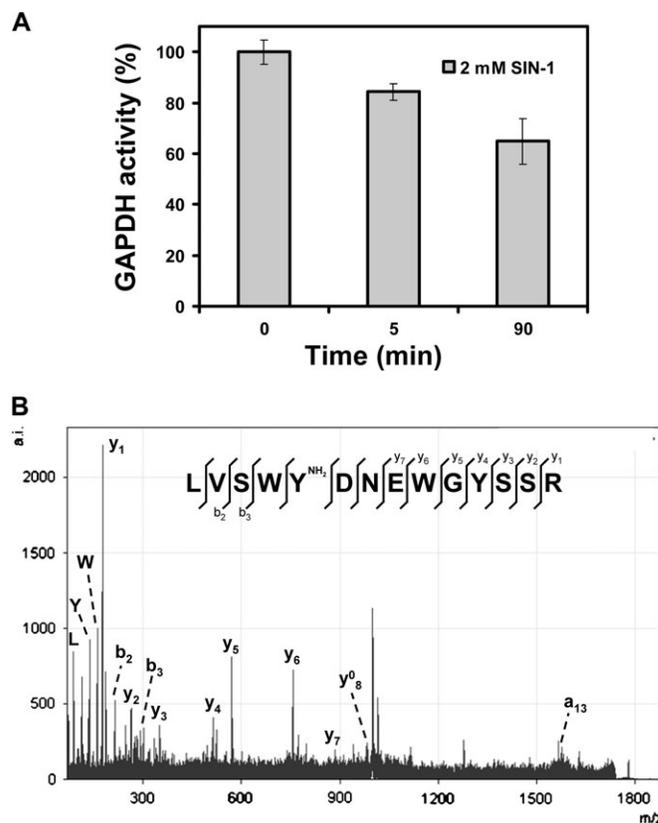

Fig. 3. Effect of nitration on GAPDH. (A) *Arabidopsis* seedlings were treated with SIN-1. After the indicated times, the GAPDH activity levels were measured in crude protein extracts from whole seedlings as described in the Materials and methods. Measurements for activity were performed in triplicate and the average values ±SD are shown. (B) MS/MS spectrum of aminated LVSWYDNEWGYSSR peptide from *Arabidopsis* glyceraldehyde-3-phosphate dehydrogenase. Detected peaks of y and b series as well as immonium ions of L, Y, and W are indicated.
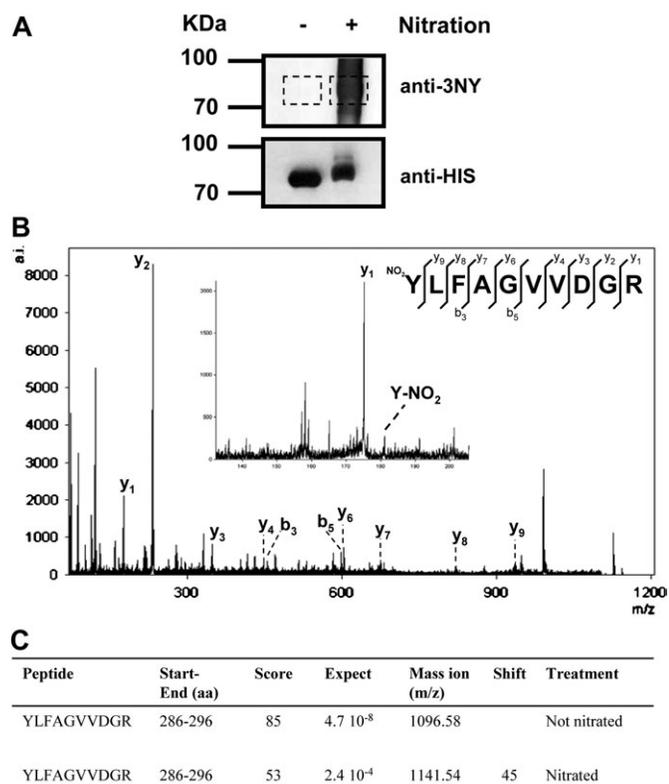
Fig. 4. Identification of the nitration site in recombinant tagged methionine synthase 1 from *Arabidopsis*. (A) Equal amounts (5 µg) of recombinant AtMS1 protein were nitrated (+) or not (–), separated by one-dimensional SDS–PAGE, and blotted onto nitrocellulose to be probed by western blot with anti-3-nitroY (anti-3NY) antibodies. After stripping, membranes were further probed with anti-5×His antibodies. Molecular size markers are shown on the left side of the panels. (B) MS/MS spectrum of nitrated YLFAGVVDGR peptide from AtMS1. The insert shows the detected y and b series as well as a detail of the spectrum showing the immonium ion corresponding to nitrated Y (C).

the bands corresponding to nitrated and non-nitrated proteins were excised from the gel, digested in gel with trypsin, and further analysed by LC-MS/MS. The same YLFAGVVDGR peptide was found from control non-nitrated protein (m/z 1096.58, score 85) and nitrated protein (m/z 1141.54, score 53), showing a shift of 44.96 equivalent to the typical shift of a single nitration (Fig. 4C). The MS/MS spectrum of nitrated peptide showed most of the peaks corresponding to the y and b series and also the immonium ion of a nitrated Y287 residue (Fig. 4B). These data allowed identification of an unequivocal site of nitration in AtMS1 at Y287. Whether this post-translational modification of AtMS1 may alter its activity, stability, subcellular location, or other post-translational modifications will require further study. Nevertheless, Y287 is conserved in plant methionine synthases but not in the enzymes from yeast (Supplementary Fig. S2A at *JXB* online), and it is located in a loop on the external surface of the protein far from the 5-methyl tetrahydropteroyltriglutamate (THG)- and homocysteine (HC)-binding sites inside the catalytic pocket (Supplementary Fig. S2B). Y287 forms hydrogen bonds with two

proximal residues, T262 and F264, which may be important to maintain suitable folding of the protein but which do not interfere directly with substrate binding or cofactor function. However, it has been described that methionine synthase activity is regulated by NO. NO treatment impairs methionine synthase activity in different models both *in vitro* (Brouwer *et al.*, 1996, Nicolaou *et al.*, 1996, 1997) and *in vivo* (Danishpajooh *et al.*, 2001), suggesting that tyrosine nitration might be responsible for the NO-dependent reduction of methionine synthase activity.

Discussion

Although several reports regarding proteomic approaches for the identification of nitrated proteins in mammals have been published recently (Suzuki *et al.*, 2005; Sultana *et al.*, 2006; Hong *et al.*, 2007; Zhang *et al.*, 2007) and the detection of nitrated proteins in pathogen-challenged plants was also reported (Romero-Puertas *et al.*, 2007), the first two reports focusing on general proteomic approaches to nitrated plant protein identification were not published until very recently (Cecconi *et al.*, 2009; Chaki *et al.*, 2009). Both groups described the use of anti-3-nitroY antibodies for the detection of plant putatively nitrated proteins in western blot and the subsequent identification of the immunoreactive proteins by MALDI-TOF/TOF. A total of 8 and 21 proteins were identified in these reports (Cecconi *et al.*, 2009; Chaki *et al.*, 2009), respectively. However, no nitrated peptides and consequently no nitration sites were identified in either of those reports, probably due to the low level of nitration under non-stressed conditions (Chaki *et al.*, 2009) and technical limitations (Cecconi *et al.*, 2009), as described by the authors. In this work, a proteomic methodology has been used to purify and identify proteins nitrated *in vivo* at Y residues in *A. thaliana*. The method is based on the purification of nitrated proteins by immunoprecipitation with well characterized anti-3-nitroY antibodies (Schmidt *et al.*, 2003; Gokulrangan *et al.*, 2007), and further identification by LC-MS/MS. This method has been previously reported to be useful in identifying nitrated proteins in mammals (Turko *et al.*, 2003; Liu *et al.*, 2009; Zhan and Desiderio, 2009). The procedure was sensitive enough to identify 127 potentially nitrated proteins from *Arabidopsis* seedlings. These results are in the range of the best proteomic methods reported in animal systems (Suzuki *et al.*, 2005; Sultana *et al.*, 2006; Hong *et al.*, 2007; Zhang *et al.*, 2007), and they represent the description of the widest potential *in vivo* nitroproteome of a plant to date. A literature search showed that ~35% of the identified *Arabidopsis* Y-nitrated proteins were previously described as Y nitrated in other organisms (Supplementary Table S1, and references therein), which supports the reliability of the method in identifying potentially Y-nitrated proteins. Moreover, a large proportion of the proteins reported to be potential targets of nitration in the two previous reports on plants (Cecconi *et al.*, 2009; Chaki *et al.*, 2009) were also identified as putatively nitrated in the present work. Moreover, some

of the MS-based protein identifications used have been technically validated by detection of the corresponding proteins in the immunopurified samples by western blot with specific antibodies (Fig. 2). Although the methodology presented in this work seems to be reliable and robust enough to be considered a good starting point for the characterization of Y-nitrated plant proteins, no un-equivocal nitration sites were found by MS/MS. Due to the low abundance of Y residues in proteins and because the nitration sites were usually restricted to one or two Y residues per protein (Abello *et al.*, 2009), a low level of occurrence of Y nitration is expected.

The most abundant protein spots in 2-DE gels from anti-3-nitroY-immunoprecipitated proteins were analysed and searched for Y nitration modification. Nitrated peptides for GAPDH, ribulose bisphosphate carboxylase large subunit, Rubisco activase, mannitol dehydrogenase, and transketolase were identified (Table 2). The identifications are based on peptide mass fingerprinting data obtained by MALDI-TOF because no good fragmentation MS/MS spectra were obtained. Only molecular ions with a signal-to-noise ratio >25 and a difference between the experimental and calculated masses of <0.15 were selected. Furthermore, *in silico* analysis of potentially nitrated peptides showed that most of them fulfilled most of the criteria to be nitration targets: Y residues were located in loops with a large solvent-accessible area and had a basic amino acid in the vicinity and a proximal negative charge (Table 3). Gene Ontology tools for the analysis of the potentially Y-nitrated identified proteins showed a significant over-representation of proteins located in the chloroplast, peroxisome, mitochondria, and apoplast, subcellular compartments that have been proposed as a source of NO and superoxide anions in plants (Corpas *et al.*, 2001; Bethke *et al.*, 2004; Gupta *et al.*, 2005; Jasid *et al.*, 2006; Flores-Pérez *et al.*, 2008; Igamberdiev and Hill, 2009), thus representing cellular domains where the nitrating reagent peroxynitrite is produced (Szabó *et al.*, 2007). These data support the previously proposed idea that the proximity of proteins to the site of generation of nitrating agents is a main factor in directing protein nitration (Ischiropoulos, 2003).

When the Gene Ontology tools were used for the analysis of the Y-nitrated identified proteins, it was found that >60% were involved in primary metabolism. Post-translational nitration of key enzymes and the subsequent alteration of their catalytic properties may represent a new level of regulation of primary metabolism. It is noteworthy that one of the proteins identified as putatively nitrated in this work (*S*-adenosyl homocysteine hydrolase, Table 1) has also been reported to be nitrated in sunflower hypocotyls (Chaki *et al.*, 2009). The activity of the enzyme was inhibited upon nitration (Chaki *et al.*, 2009), thus suggesting that the activity of the *Arabidopsis* counterpart may also be regulated through nitration. Moreover, Rubisco activase, ATP synthase subunit α, and glutamine synthetase 2 have also been identified as putative nitrated proteins in pathogen-challenged *Arabidopsis* (Cecconi *et al.*, 2009). It has been discussed that nitration of these proteins may be a way to

modulate defence-related responses including the hypersensitive response (Cecconi *et al.*, 2009). Alternatively, nitration of abundant proteins such as those involved in photosynthesis and carbon metabolism may represent just a non-selective scavenging system for reactive nitrogen and oxygen species produced under standard or stress-related conditions. Moreover, the functional relevance of this post-translational modification on these targets is further supported by the fact that most of the identified nitrated Y residues are strictly conserved in the amino acid sequence of homologous proteins from other organisms (Supplementary Fig. S1 at *JXB* online), thus supporting a potential functional effect of this post-translational modification.

In the case of GADPH, the two Y residues identified as nitrated in peptide LVSWY*DNEWGY*SSR were not only conserved in the rabbit GAPDH but were actually also identified as nitrated LISWY*DNEFGY*SNR, resulting in complete loss of catalytic activity (Palamalai and Miyagi, 2010). GAPDH models for rat and *Arabidopsis* overlapped greatly throughout the molecule and particularly on nitrated Y residues (Supplementary Fig. S3). In addition, as reported for yeast and mammals (Buchczyk *et al.*, 2000; Palamalai and Miyagi, 2010), *Arabidopsis* GAPDH activity was also inhibited by peroxynitrite (Fig. 3A). Notwithstanding, several proteins participating with GAPDH in the gluconeogenesis conversion of malate to sucrose were also identified as nitrated forms in *Arabidopsis* (Table 1 and Supplementary Fig. S4), thus suggesting a potential for Y nitration as a significant regulatory level on this principal metabolic pathway. Interestingly, among potential targets of Y nitration in *Arabidopsis* were also three enzymes involved in the biosynthesis of methionine, the 5-methyl tetrahydropteroyltriglutamate-homocysteine methyltransferase, also called methionine synthase, the *S*-adenosylmethionine synthetases 1 and 2, and *S*-adenosylhomocysteinase 1 (Supplementary Fig. S4). It has been previously reported that NO probably inhibits mammalian methionine synthase activity by reaction with cobalt-containing cobalamin cofactor (Brouwer *et al.*, 1996; Nicolaou *et al.*, 1997; Danishpajooh *et al.*, 2001). Nevertheless, in the light of the results obtained here, this mode of action for NO is compatible with the mechanism of control of methionine synthase activity through nitration of key Y residues of the protein. Moreover, the fact that not only a key regulatory step but most of the enzymes involved in methionine biosynthesis are potentially nitrated in *Arabidopsis* suggests that Y nitration may represent an important regulatory level to control the biosynthesis of this amino acid in plants. Furthermore, nitration of *S*-adenosylmethionine synthetases could also represent an interesting regulatory point in ethylene production. Regarding this, the *S*-nitrosylation of *S*-adenosylmethionine synthetase 1 resulting in reduced activity and decreased ethylene production in *Arabidopsis* has recently been reported (Lindermayr *et al.* 2006).

The fact that neither in this work nor in the two previous reports on protein nitration in plants (Cecconi *et al.*, 2009; Chaki *et al.*, 2009) were any nitrated peptide and the corresponding nitration site unequivocally identified needs further discussion. It is well known that Y nitration is a very

low abundant post-translational modification as compared with other protein modifications such as phosphorylation (Abello *et al.*, 2009). In fact, only 0.033–0.43 mmol of nitroY per mol of Y has been detected in plant proteins, depending on the tissue or species studied (Bechtold *et al.*, 2009; Chaki *et al.*, 2009). Moreover, it is also likely that under non-stressed conditions, when only basal levels of NO and superoxide and thus low amounts of peroxynitrite are generated by cells, even lower abundance is expected. Nevertheless, because the presented methodology enriched samples in potentially Y-nitrated-containing proteins by immunoprecipitation with a specific anti-3-nitroY antibody, the identification of some nitrated peptides by MS/MS should be expected. A survey of the literature on identification of nitrated proteins in different organisms points to a very low number of nitrated sites identified, thus suggesting the existence of technical difficulties intrinsically associated with MS-based analysis of this kind of protein modification. A possible explanation for the lack of nitroY signatures could be related to alterations produced by the treatments performed before mass spectrometry analysis or during the ionization of the protein samples. It has been reported that the treatment of nitrated proteins with DTT and elevated temperature, as used for trypsin digestion, can reduce the nitroY to aminoY or other related species (Söderling *et al.*, 2007). Moreover, the ionization energy for MALDI or electrospray ionization (ESI) technologies is too aggressive for the nitrated Y residues, and the laser-induced photochemical decomposition of nitroY to aminoY during MALDI-MS analysis has been reported (Sarver *et al.*, 2001). Therefore, a conversion of nitroY to aminoY in the samples during sample processing before MS analysis may explain the lack of detection of nitrated peptides in the present studies. To validate this hypothesis, the proteomic experiments were searched for aminoY modification instead of nitroY modification. By selecting aminoY as a variable modification in the MASCOT data analysis in MALDI-TOF/TOF experiments, a fragmentation MS/MS spectrum corresponding to a peptide containing a 3-aminoY residue was found in the protein spot corresponding to GADPH (Fig. 3). More precisely a peptide containing aminoY318 was found, suggesting that from the two Y residues found as potential targets to be nitrated in G3PC (Table 2), part of the 3-nitroY318 residues in the protein population might undergo reduction to 3-aminoY318 under the conditions used for MS analysis. Moreover, although no further MS/MS spectra corresponding to aminoY-containing peptides were obtained, ~50 additional putative aminoY-containing peptides with an ion score >15 were found (Supplementary Table S3 at *JXB* online). This confirms the hypothesis that the lack of identification of nitrated peptides in this work, and probably in others, may be due to the conversion of the nitroY to aminoY. Such a conclusion leads to the proposal that future analysis of Y nitration of proteins should be based on a simultaneous search for both nitroY and aminoY variable modifications. Eventually, the chemical reduction of all nitroY to aminoY by means of a strong reducing reagent such as sodium dithionite may represent an advantage in

further proteomic analysis either searching directly for aminoY or after derivatization of aminoY (Ghesquière *et al.*, 2009; Abello *et al.*, 2010).

The proteomic method described in this work represents a tool to identify proteins undergoing *in vivo* Y nitration in plants. The application of this methodology, with the improvements discussed above, to the analysis of different biological processes in plants will allow the identification of Y nitration protein targets. Because of the low abundance and limited stability of this post-translational modification, the obtained data suggest that after identification of *in vivo* targets, the confirmation of the modification sites and the functional consequences have to be addressed through *in vitro* assays with larger amounts of modified protein. These Y-nitrated proteins may represent nodes for a new unexplored level of regulation of proteins exerted by NO through post-translational modification. Further characterization of the identified Y-nitrated proteins will provide key information about new regulatory features of NO in many aspects of plant growth, development, and defence.

Supplementary data

Supplementary data are available at *JXB* online.

Figure S1. Potential Y nitration targets in glyceraldehyde-3-phopsphate dehydrogenase, serine hydroxymethyltransferase, transketolase, Rubisco large subunit, and Rubisco activase are conserved in different plants and other organisms.

Figure S2. Conservation and structural modelling analysis of plant methionine synthases.

Figure S3. Alignment of 3D structure models of rat and *Arabidopsis* glyceraldehyde-3-phosphate dehydrogenases.

Figure S4. Scheme displaying primary carbon and sulphur metabolism enzymes highlighting those that have been identified in this work as potentially nitrated in *Arabidopsis*.

Figure S5. Confirmation of the presence of proteins identified through shotgun proteomic analysis in the immnunopurified nitroproteome. The entire gels for western blots performed in Fig. 2 are shown to account for the specificity of the antibodies.

Figure S6. ROS and NO detection in roots of wild-type plants grown under standard conditions. Nitroblue tetrazolium (NBT) staining of roots in different zones (A, B). Roots were pre-incubated with 10 U ml^{-1} superoxide dismutase (SOD) prior to NBT staining (C, D). DAF-FM DA staining of roots pre-treated (G, H) or not (E, F) with the NO scavenger cPTIO under UV illumination (E, G) or bright field (F, H).

Table S1. Putative Y-nitrated proteins identified from *Arabidopsis* and the corresponding functional Y-nitrated counterparts in other organisms.

Table S2. Identification of potentially Y-nitrated proteins by MALDI-TOF peptide fingerprinting of the most abundant 2D gel-excised spots from anti-3-nitroY-immunoprecipitated *Arabidopsis* proteins.

Table S3. Identification of potential targets of 3-aminoY modification by shotgun LC-MS/MS analysis.

References

Abello N, Barroso B, Kerstjens HA, Postma DS, Bischoff R. 2010. Chemical labeling and enrichment of nitrotyrosine-containing peptides. *Talanta* **80,** 1503–1512.

Abello N, Kerstjens HA, Postma DS, Bischoff R. 2009. Protein tyrosine nitration: selectivity, physicochemical and biological consequences, denitration, and proteomics methods for the identification of tyrosine-nitrated proteins. *Journal of Proteome Research* **8,** 3222–3328.

Arnold K, Bordoli L, Kopp J, Schwede T. 2006. The SWISS-MODEL workspace: a web-based environment for protein structure homology modelling. *Bioinformatics* **22,** 195–201.

Bechtold U, Rabbani N, Mullineaux PM, Thornalley PJ. 2009. Quantitative measurement of specific biomarkers for protein oxidation, nitration and glycation in Arabidopsis leaves. *The Plant Journal* **59,** 661–671.

Bethke PC, Badger MR, Jones RL. 2004. Apoplastic synthesis of nitric oxide by plant tissues. *The Plant Cell* **16,** 332–41.

Bethke PC, Libourel IG, Jones RL. 2006. Nitric oxide reduces seed dormancy in Arabidopsis. *Journal of Experimental Botany* **57,** 517–526.

Bowie JU, Lüthy R, Eisenberg D. 1991. A method to identify protein sequences that fold into a known three-dimensional structure. *Science* **253,** 164–170.

Brouwer M, Chamulitrat W, Ferruzzi G, Sauls DL, Weinberg JB. 1996. Nitric oxide interactions with cobalamins: biochemical and functional consequences. *Blood* **88,** 1857–1864.

Buchczyk DP, Briviba K, Hartl FU, Sies H. 2000. Responses to peroxynitrite in yeast: glyceraldehyde-3-phosphate dehydrogenase (GAPDH) as a sensitive intracellular target for nitration and enhancement of chaperone expression and ubiquitination. *Biological Chemistry* **381,** 121–126.

Cecconi D, Orzetti S, Vandelle E, Rinalducci S, Zolla L, Delledonne M. 2009. Protein nitration during defense response in *Arabidopsis thaliana. Electrophoresis* **30,** 2460–2468.

Chaki M, Valderrama R, Fernández-Ocaña AM, et al. 2009. Protein targets of tyrosine nitration in sunflower (*Helianthus annuus* L.) hypocotyls. *Journal of Experimental Botany* **60,** 4221–4234.

Chang GG, Huang TM. 1980. Involvement of tyrosyl residues in the substrate binding of pigeon liver malic enzyme. *Biochimica et Biophysica Acta* **611,** 217–226.

Chen H-JC, Chang C-M, Lin W-P, Cheng D-L, Leong M-I. 2008. H2O2/nitrite-induced post-translational modifications of human hemoglobin determined by mass spectometry: redox regulation of tyrosine nitration and 3-nitrotyrosine reductions by antioxidants. *Chembiochem* **9,** 312–323.

Chiappetta G, Corbo C, Palmese A, Galli F, Piroddi M, Marino G, Amoresano A. 2009. Quantitative identification of protein nitration sites. *Proteomics* **9,** 1524–1537.

Corpas FJ, Barroso JB, del Río LA. 2001. Peroxisomes as a source of reactive oxygen species and nitric oxide signal molecules in plant cells. *Trends in Plant Science* **6,** 145–150.

Danishpajooh IO, Gudi T, Chen Y, Kharitonov VG, Sharma VS, Boss GR. 2001. Nitric oxide inhibits methionine synthase activity *in vivo* and disrupts carbon flow through the folate pathway. *Journal of Biological Chemistry.* **20,** 27296–27303.

Dixon DP, Skipsey M, Grundy NM, Edwards R. 2005. Stress-induced protein S-glutathionylation in Arabidopsis. *Plant Physiology* **138,** 2233–2244.

Flores-Pérez U, Sauret-Güeto S, Gas E, Jarvis P, Rodríguez-Concepción M. 2008. A mutant impaired in the production of plastome-encoded proteins uncovers a mechanism for the homeostasis of isoprenoid biosynthetic enzymes in Arabidopsis plastids. *The Plant Cell* **20,** 1303–1315.

Ghesquière B, Colaert N, Helsens K, et al. 2009. *In vitro* and *in vivo* protein-bound tyrosine nitration characterized by diagonal chromatography. *Molecular and Cellular Proteomics* **8,** 2642–2652.

Gokulrangan G, Zaidi A, Michaelis ML, Schöneich C. 2007. Proteomic analysis of protein nitration in rat cerebellum: effect of biological aging. *Journal of Neurochemistry* **100,** 1494–1504.

Gow AJ, Farkouh CR, Munson DA, Posencheg MA, Ischiropoulos H. 2004. Biological significance of nitric oxide-mediated protein modifications. *American Journal of Physiology: Lung Cellular and Molecular Physiology* **287,** L262–L268.

Grün S, Lindermayr C, Sell S, Durner J. 2006. Nitric oxide and gene regulation in plants. *Journal of Experimental Botany* **57,** 507–516.

Gupta KJ, Stoimenova M, Kaiser WM. 2005. In higher plants, only root mitochondria, but not leaf mitochondria reduce nitrite to NO, *in vitro* and *in situ. Journal of Experimental Botany* **56,** 2601–2609.

He Y, Tang RH, Hao Y, et al. 2004. Nitric oxide represses the Arabidopsis floral transition. *Science* **305,** 1968–1971.

Hong SJ, Gokulrangan G, Schöneich C. 2007. Proteomic analysis of age dependent nitration of rat cardiac proteins by solution isoelectric focusing coupled to nanoHPLC tandem mass spectrometry. *Experimental Gerontology* **42,** 639–651.

Igamberdiev AU, Hill RD. 2009. Plant mitochondrial function during anaerobiosis. *Annals of Botany* **103,** 259–268.

Ischiropoulos H. 2003. Biological selectivity and functional aspects of protein tyrosine nitration. *Biochemical and Biophysical Research Communication* **305,** 776–783.

Jasid S, Simontacchi M, Bartoli CG, Puntarulo S. 2006. Chloroplasts as a nitric oxide cellular source. Effect of reactive nitrogen species on chloroplastic lipids and proteins. *Plant Physiology* **142,** 1246–1255.

Laskowski RA, Rullmannn JA, MacArthur MW, Kaptein R, Thornton JM. 1996. AQUA and PROCHECK-NMR: programs for checking the quality of protein structures solved by NMR. *Journal of Biomolecular NMR* **8,** 477–486.

Lindermayr C, Saalbach G, Bahnweg G, Durner J. 2006. Differential inhibition of Arabidopsis methionine adenosyltransferases by protein S-nitrosylation. *Journal of Biological Chemistry* **281,** 4285–4291.

Lindermayr C, Saalbach G, Durner J. 2005. Proteomic identification of S-nitrosylated proteins in Arabidopsis. *Plant Physiology* **137,** 921–930.

Liu B, Tewari AK, Zhang L, Green-Church KB, Zweier JL, Chen YR, He G. 2009. Proteomic analysis of protein tyrosine nitration after ischemia reperfusion injury: mitochondria as the major target. *Biochimica et Biophysica Acta* **1794,** 476–485.

Liu HY, Yu X, Cui DY, Sun MH, Sun WN, Tang ZC, Kwak SS, Su WA. 2007. The role of water channel proteins and nitric oxide signaling in rice seed germination. *Cell Research* **17,** 638–649.

Melo F, Feytmans E. 1998. Assessing protein structures with a non-local atomic interaction energy. *Journal of Molecular Biology* **277,** 1141–1152.

Mishina TE, Lamb C, Zeier J. 2007. Expression of a nitric oxide degrading enzyme induces a senescence programme in Arabidopsis. *Plant, Cell and Environment* **30,** 39–52.

Miyagi M, Sakaguchi H, Darrow RM, Yan L, West KA, Aulak KS, Stuehr DJ, Hollyfield JG, Organisciak DT, Crabb JW. 2002. Evidence that light modulates protein nitration in rat retina. *Molecular and Cellular Proteomics* **1,** 293–303.

Morot-Gaudry-Talarmain Y, Rockel P, Moureaux T, Quilleré I, Leydecker MT, Kaiser WM, Morot-Gaudry JF. 2002. Nitrite accumulation and nitric oxide emission in relation to cellular signaling in nitrite reductase antisense tobacco. *Planta* **215,** 708–715.

Muñoz-Bertomeu J, Cascales-Miñana B, Mulet JM, Baroja-Fernández E, Pozueta-Romero J, Kuhn JM, Segura J, Ros R. 2009. Plastidial glyceraldehyde-3-phosphate dehydrogenase deficiency leads to altered root development and affects the sugar and amino acid balance in Arabidopsis. *Plant Physiology* **151,** 541–558.

Mur LA, Carver TL, Prats E. 2006. NO way to live; the various roles of nitric oxide in plant–pathogen interactions. *Journal of Experimental Botany* **57,** 489–505.

Nicolaou A, Kenyon SH, Gibbons JM, Ast T, Gibbons WA. 1996. *In vitro* inactivation of mammalian methionine synthase by nitric oxide. *European Journal of Clinical Investigation* **26,** 167–170.

Nicolaou A, Warefield CJ, Kenyon SH, Gibbons WA. 1997. The inactivation of methionine synthase in isolated rat hepatocytes by sodium nitroprusside. *European Journal of Biochemisyry* **244,** 876–882.

Palamalai V, Miyagi M. 2010. Mechanism of glyceraldehyde-3-phosphate dehydrogenase inactivation by tyrosine nitration. *Protein Science* **19,** 255–262.

Parani M, Rudrabhatla S, Myers R, Weirich H, Smith B, Leaman DW, Goldman SL. 2004. Microarray analysis of nitric oxide responsive transcripts in Arabidopsis. *Plant Biotechnology Journal* **2,** 359–366.

Petersen B, Petersen TN, Andersen P, Nielsen M, Lundegaard C. 2009. A generic method for assignment of reliability scores applied to solvent accessibility predictions. *BMC Structural Biology* **9,** 51.

Polverari A, Molesini B, Pezzotti M, Buonaurio R, Marte M, Delledonne M. 2003. Nitric oxide-mediated transcriptional changes in *Arabidopsis thaliana. Molecular Plant-Microbe Interactions* **16,** 1094–1105.

Romero-Puertas MC, Campostrini N, Mattè A, Righetti PG, Perazzolli M, Zolla L, Roepstorff P, Delledonne M. 2008. Proteomic analysis of S-nitrosylated proteins in Arabidopsis thaliana undergoing hypersensitive response. *Proteomics* **8,** 1459–1469.

Romero-Puertas MC, Laxa M, Mattè A, Zaninotto F, Finkemeier I, Jones AM, Perazzolli M, Vandelle E, Dietz KJ, Delledonne M. 2007. S-nitrosylation of peroxiredoxin II E promotes peroxynitrite-mediated tyrosine nitration. *The Plant Cell* **19,** 4120–30.

Romero-Puertas MC, Perazzolli M, Zago ED, Delledonne M. 2004. Nitric oxide signalling functions in plant–pathogen interactions. *Cell Microbiology* **6,** 795–803.

Saito S, Yamamoto-Katou A, Yoshioka H, Doke N, Kawakita K. 2006. Peroxynitrite generation and tyrosine nitration in defense responses in tobacco BY-2 cells. *Plant and Cell Physiology* **47,** 689–697.

Sarver A, Scheffler NK, Shetlar MD, Gibson BW. 2001. Analysis of peptides and proteins containing nitrotyrosine by matrix-assisted laser desorption/ionization mass spectrometry. *Journal of the American Society of Mass Spectrometry* **12,** 439–448.

Schmidt P, Youhnovski N, Daiber A, Balan A, Arsic M, Bachschmid M, Przybylski M, Ullrich V. 2003. Specific nitration at tyrosine 430 revealed by high resolution mass spectrometry as basis for redox regulation of bovine prostacyclin synthase. *Journal of Biological Chemistry* **278,** 12813–12819.

Simpson GG. 2005. NO flowering. *Bioessays* **27,** 239–241.

Söderling AS, Hultman L, Delbro D, Højrup P, Caidahl K. 2007. Reduction of the nitro group during sample preparation may cause underestimation of the nitration level in 3-nitrotyrosine immunoblotting. *Journal of Chromatography B* **851,** 277–286.

Souza JM, Daikhin E, Yudkoff M, Raman CS, Ischiropoulos H. 1999. Factors determining the selectivity of protein tyrosine nitration. *Archives of Biochemistry and Biophysics* **371,** 169–178.

Stevens SM Jr, Prokai-Tatrai K, Prokai L. 2008. Factors that contribute to the misidentification of tyrosine nitration by shotgun proteomics. *Molecular and Cellular Proteomics* **7,** 2442–2451.

Sultana R, Poon HF, Cai J, Pierce WM, Merchant M, Klein JB, Markesbery WR, Butterfield DA. 2006. Identification of nitrated proteins in Alzheimer's disease brain using a redox proteomics approach. *Neurobiology of Disease* **22,** 76–87.

Suzuki Y, Tanaka M, Sohmiya M, Ichinose S, Omori A, Okamoto K. 2005. Identification of nitrated proteins in the normal rat brain using a proteomics approach. *Neurological Research* **27,** 630–633.

Szabó C, Ischiropoulos H, Radi R. 2007. Peroxynitrite: biochemistry, pathophysiology and development of therapeutics. *Nature Reviews on Drug Discovery* **6,** 662–680.

Tsumoto H, Taguchi R, Kohda K. 2010. Efficient identification and quantification of peptides containing nitrotyrosine by matrix-assisted laser desorption/ionization time-of-flight mass spectrometry after derivatization. *Chemical and Pharmaceutical Bulletin* **58,** 488–494.

Turko IV, Li L, Aulak KS, Stuehr DJ, Chang JY, Murad F. 2003. Protein tyrosine nitration in the mitochondria from diabetic mouse heart. Implications to dysfunctional mitochondria in diabetes. *Journal of Biological Chemistry* **278,** 33972–33977.

Zhan X, Desiderio DM. 2009. Mass spectrometric identification of *in vivo* nitrotyrosine sites in the human pituitary tumor proteome. *Methods in Molecular Biology* **566,** 137–163.

Zhang Q, Qian WJ, Knyushko TV, et al. 2007. A method for selective enrichment and analysis of nitrotyrosine-containing peptides in complex proteome samples. *Journal of Proteome Research* **6,** 2257–2268.

Zhang Y, Wang L, Liu Y, Zhang Q, Wei Q, Zhang W. 2006. Nitric oxide enhances salt tolerance in maize seedlings through increasing activities of proton-pump and Na+/H+ antiport in the tonoplast. *Planta* **224,** 545–555.